Am J Cancer Res 2022;12(7):3223-3241
www.ajcr.us /ISSN:2156-6976/ajcr0144231

Original Article

MIR133A regulates cell proliferation, migration, and apoptosis by targeting SOX9 in human colorectal cancer cells

Santosh Lamichhane[1], Ji-Su Mo[2], Grinsun Sharma[1], Sun-Myoung Joung[1], Soo-Cheon Chae[1,2]

[1]*Department of Pathology, School of Medicine, Wonkwang University, Iksan, Chonbuk 54538, Korea;* [2]*Digestive Disease Research Institute, Wonkwang University, Iksan, Chonbuk 54538, Korea*

Received May 17, 2022; Accepted June 18, 2022; Epub July 15, 2022; Published July 30, 2022

Abstract: The human microRNA 133A (*MIR133A*) was identified as a CRC-associated miRNA. It was down-regulated in human CRC tissues. We identified the putative *MIR133A1* and *A2* target genes by comparing the transcriptome analysis data of *MIR133A1* and *A2* knock-in cells with the candidate *MIR133A* target genes predicted by bioinformatics tools. We identified 29 and 33 putative *MIR133A* and *A2* direct target genes, respectively. Among them, we focused on the master transcription regulator gene SRY-box transcription factor 9 (*SOX9*), which exhibits a pleiotropic role in cancer. We confirmed that *SOX9* is a direct target gene of *MIR133A* by luciferase reporter assay, quantitative RT-PCR, and western blot analysis. Overexpression of *MIR133A* in CRC cell lines significantly decreased SOX9 and its downstream PIK3CA-AKT1-GSK3B-CTNNB1 and KRAS-BRAF-MAP2K1-MAPK1/3 pathways and increased apoptosis. Furthermore, functional studies reveal that cell proliferation, colony formation, and migration ability were significantly decreased by *MIR133A*-overexpressed CRC cell lines. Knockdown of SOX9 in CRC cell lines by *SOX9* gene silencing showed similar results. We also used a xenograft model to show that *MIR133A* overexpression suppresses tumor growth and proliferation. Our results suggest that *MIR133A* regulates cell proliferation, migration, and apoptosis by targeting *SOX9* in human colorectal cancer.

Keywords: *MIR133A*, SOX9, cell proliferation, apoptosis, colorectal cancer

Introduction

Colorectal cancer (CRC) is a common public health issue and a lethal disease, increasingly affecting the population of highly developed countries [1]. Over the last four decades, the prevalence of CRC has climbed at an alarming rate. In 2020, 1.9 million new CRC cases and 0.9 million deaths were reported, accounting for almost 10% of all new cancer cases and deaths worldwide [2, 3]. Several meticulous scientific studies have revealed that genetic variation, epigenetic modification, age, diet, smoking, drinking, microbiome, sedentary lifestyle, and environmental factors cause CRC [4, 5]. Multimodal treatment approaches, such as surgical resection combined with chemotherapy and radiotherapy, are routinely used as conventional therapies for people with CRC. However, due to the formation of CRC chemoresistance, toxicity, and other unfavorable side effects, the clinical outcome of advanced-stage illness remains gloomy [6]. Hence, it is necessary to develop new strategies to overcome these limits. miRNA-based gene therapy is becoming a new strategy for cancer treatment because it has been found that many miRNA target sites are localized in cancer-associated genomic regions [7, 8]. It is believed that CRC is a genetically susceptible disease, and estimates are that between 25% and 50% of CRCs show some familial predisposition [9]. However, the complete set of colorectal cancer driver genes, including their contributions to hereditary disease susceptibility and underlying mechanisms of action, has yet to be fully described.

MicroRNAs are short (19-25 nucleotides), noncoding, endogenous, single-stranded RNAs that bind to the 3'-untranslated region (3'-UTR) of their target mRNA and can repress mRNA translation or induce mRNA degradation by cleav-

age of the target mRNA [8]. These master gene regulators (miRNAs) affect the pathogenesis of various cancer types by functioning as oncogenes or tumor suppressor genes and are significantly involved in critical events of carcinogenesis [10, 11]. Endogenous miRNAs regulate more than 50% of human genes, and their abnormal expression causes various biological modifications such as apoptosis, cell differentiation, proliferation, migration, invasion, and angiogenesis [11, 12]. According to miRNA genomic expression profiling studies, *MIR133A* is aberrantly expressed in several tissues or organs and has been confirmed as a tumor suppressor in various cancers, including CRC, by suppressing cell proliferation, metastasis, migration, and invasion [13, 14]. Conversely, there are some reports that dispute *MIR133A*'s role in CRC initiation, tumorigenesis, and metastasis, and it was persistently up-regulated in human airway epithelial cells, contributing to epithelial-mesenchymal transition (EMT) of cancer [15]. Likewise, a study reported that *MIR133A* was upregulated along with *MIR1* in multiple myeloma compared to normal samples using microarrays [16].

SRY-box transcription factor 9 (SOX9) is a DNA-binding high mobility group (HMG) transactivation domain that plays a crucial role in the development and progression of various diseases, including cancer [17, 18]. Like other proteins, SOX9 is regulated by post-transcriptional and post-translation modifications like microRNA binding, DNA methylation, acetylation, phosphorylation, and ubiquitination at different amino acid sequences [19]. Over the last few years, increasing evidence has suggested that SOX9 regulates diverse cellular processes, including cell proliferation, metastasis, migration, apoptosis, and invasion [20, 21]. Interestingly, some researchers have defined *SOX9* as an oncogene [22, 23], while others argue that it is a tumor suppressor gene [24]. Therefore, the detailed underlying mechanisms need to be further elucidated.

Consequently, in this study, we speculate on the specific function of *MIR133A* in CRC, which might be helpful to identify novel therapeutic targets and strategies to manage cancer. In this study, we found that *MIR133A* is significantly downregulated in CRC tissues and *SOX9* is a direct target of *MIR133A* in human CRC cells. We demonstrated that *MIR133A* regulates cell proliferation, colony formation and migration ability by suppressing the *SOX9* pathway.

Material and methods

Patients and human samples

The tissue samples used in this study were provided by the Biobank of Wonkwang University Hospital, a member of the National Biobank of Korea. With approval from the Institutional Review Board and informed consent from the subjects (WKIRB-202006-BR-023), we obtained CRC tissues from 10 colon cancer patients: 6 samples from tumor stage 3 (5 females, 1 male) and the remaining 4 samples from tumor stage 4 (3 females, 1 male). The mean ages of colon and rectal cancer patients were 64.2 and 72.1 years, respectively. Six separate colon cancer tissue samples and matched normal colon tissue samples (T3, females) were used to analyze endogenous *MIR133A* levels. In parallel, the remaining samples were used to evaluate SOX9 protein expression by western blotting. Additionally, 4 separate colon cancer tissue samples and matched normal colon tissue samples, 2 samples from T3 (1 male, 1 female) and 2 samples from T4 (1 male, 1 female), were used to assess in situ SOX9 expression by immunohistochemistry.

Cell culture

Human CRC cell lines (HCT116, SW48, Caco2 and SW480) were obtained from the Korea Cell Line Bank (KCLB, Seoul, Korea) or the American Type Culture Collection (ATCC, Rockville, MD, USA). The SW48, HCT116 and SW480 cells were cultured in RPMI 1640 (HyClone, Logan, UT, USA) supplemented with 10% fetal bovine serum (FBS) in 5% CO_2 at 37°C in a humidified atmosphere. The Caco2 cells were cultured in Alpha-MEM (HyClone) supplemented with 10% FBS in 5% CO_2 at 37°C in a humidified atmosphere.

Stable expression of MIR133A1 and A2 in CRC cell lines

HCT116 and SW48 cells stably expressing *MIR133A1* and *A2* were generated using the Mir-X™ Inducible miRNA system (Takara Bio, San Jose, CA, USA). HCT116 (5×10^5) and SW-48 (1×10^5) cells were then transfected with the

pTet-on Advanced plasmid using Lipofectamine 2000 (Invitrogen, Waltham, MA, USA) in 24-well plates. Stable Tet-on advanced cell lines were generated using G418 500 μg/mL (Takara Bio), and 100 μg/mL G418 was used for maintenance concentration. Primers (Table S1) were used to amplify *MIR133A1* and *A2* from human genomic DNA and the products were cloned into the pmRi-mCherry vector to form pmRi-mCheery *miRNA133A1* and *A2* expression vectors, which were then transfected into the Tet-on Advanced cell line along with one of the linear markers. CRC cells stably expressing pmRi-mCheery *miRNA133A1* (*MIR133A1* knock-in, *MIR133A1* KI) and *A2* (*MIR133A2* knock-in; *MIR133A2* KI) were selected using 1 μg/mL puromycin and further maintained in 0.5 μg/mL puromycin. Lastly, doxycycline 1 μg/mL was added to induce *MIR133A1* and *A2* expression. Stable expression of *MIR133A1* and *A2* was confirmed using TaqMan microRNA assay (Applied Biosystems, Waltham, MA, USA).

RNA extraction, miRNA and mRNA expression analysis

Total RNA was extracted from the tissue samples, cell pellets of *MIR133A*1 KI and *MIR133A2* KI cell lines or *MIR133A1*-overexpressed (*MIR133A1* mimic-transfected) cells using TRIzol reagent (Invitrogen), and RNA integrity was quantified by using RT-PCR (qRT-PCR) as previously described [11, 12, 25]. TaqMan miRNA assays were used to quantify the mature levels of *MIR133A*. The mRNA levels were quantified with qRT-PCR using SYBR Green master mixture (Applied Biosystems). RNU48 (for TaqMan qRT-PCR) and *GAPDH* were used as endogenous controls of miRNA and mRNA qRT-PCR, respectively. Each sample was run in triplicate. The primers that we used are listed in Table S1.

Transfection and oligonucleotides

The HCT116 and SW48 cells were plated on 10 cm dishes and cultured as described above. The *MIR133A* mimic (hsa-miR-133A, pre-miR miRNA precursor AM17100, product ID: PM-12946) and negative control oligonucleotides were commercially synthesized (Ambion, Austin, TX, USA) and used at 50 nmol/mL for transfections. The transfections were performed with Lipofectamine RNAiMAX (Invitrogen) or siPORT NeoFX transfection agent (Ambion) according to the manufacturers' recommendations. The *SOX9* small interfering RNA (*siSOX9*) and negative control siRNA transfections were performed according to the manufacturer's protocol (Ambion). The cells were harvested for 72 h (for protein expression) after transfection for protein analysis.

RNA sequencing (RNA-Seq) analysis in MIR133A1 KI and MIR133A2 KI cells

Total RNA was isolated from *MIR133A1* or *MIR133A2* knock-in cell lines using Trizol reagent (Invitrogen). RNA quality was assessed by Agilent 2100 bioanalyzer (Agilent Technologies, Amstelveen, the Netherlands), and RNA quantification was performed using the ND 2000 Spectrophotometer (Thermo Inc., Wilmington, DE, USA). Library preparation and sequencing libraries were prepared from total RNA using the NEBNext Ultra II Directional RNA Seq Kit (New England BioLabs, Inc., Hitchin, UK). The isolation of mRNA was performed using the Poly (A) RNA Selection Kit (Lexogen, Inc., Vienna, Austria). The isolated mRNAs were used for cDNA synthesis and shearing following manufacturer's instructions. Indexing was performed using the Illumina indexes 112. The enrichment step was carried out using PCR. Subsequently, libraries were checked using the Agilent 2100 bioanalyzer (DNA High Sensitivity Kit) to evaluate the mean fragment size. Quantification was performed using the library quantification kit using a StepOne Real-Time PCR System (Life Technologies, Inc., Carlsbad, CA, USA). High throughput sequencing was performed as paired end 100 sequencing using NovaSeq 6000 (Illumina, Inc., San Diego, CA, USA). A quality control of raw sequencing data was performed using Fast QC [26]. Adapter and low-quality reads (<Q20) were removed using FASTX Trimmer (http://hannonlab.cshl.edu/fastx_toolkit/2014) and BBMap (https://sourceforge.net/projects/bbmap/(2014)). Then the trimmed reads were mapped to the reference genome using TopHat [27]. Gene expression levels were estimated using FPKM (Fragments Per kb per Million reads) values by Cufflinks [28]. The FPKM values were normalized based on the Quantile normalization method using EdgeR within R [29]. Data mining and graphic visualization were performed using ExDEGA (ebiogen, Inc., Seoul, Korea).

Plasmid construct and luciferase reporter assay

Wild-type (WT) or mutant-type (MT) fragments of *SOX9* 3' UTR containing the predicted binding site of *MIR133A* were amplified by PCR using the primer set shown in Table S1. The PCR product was cloned into the pmirGLO Dual-Luciferase miRNA Target Expression Vector (Promega, Madison, WI, USA). The luciferase assay results were analyzed as previously described [11, 12, 30].

MTT cell viability and migration assay

To determine the effect of *MIR133A* on the cell viability of colon cancer cell lines, HCT116 (1×10^4 cells/well) and SW48 (2×10^4 cells/well) were transfected with *MIR133A* mimic (50 nM), *siSOX9*, or control in 96-well plates and incubated in humidified air containing 5% CO_2 at 37°C for the indicated time. Likewise, stable HCT116 and SW48 cells overexpressing *MIR-133A1*, *A2*, and normal control cells were seeded in 96-well plates as above, and after a 24 h incubation doxycycline (1 μg/mL) was added to all groups and incubated in an incubator. Further steps were carried out according to previous methods [31, 32].

Colony-forming assay

HCT116 (500 cells/well) and SW48 (1000 cells/well) were transfected with *MIR133A* mimic (50 nM) or control in 12-well plates and incubated in humidified air containing 5% CO_2 at 37°C for 2 or 3 weeks to allow colony formation. The media was changed every 2 or 3 days, and cells were washed with 1× PBS. Colony fixation-staining was done by adding 0.5-1 ml mixture of 0.5% crystal violet and 6% glutaraldehyde, leaving the plate for at least 30 min at room temperature (RT). After that, the glutaraldehyde crystal-violet mixture was removed and washed by dipping the plates in tap water. The plate was dried at RT and the number of colonies was counted and normalized to the control cell results.

Xenograft model

Male BALB/c nude mice (6 weeks old, 20-21 g) were purchased from Charles River Technology (Boston, MA, USA) through Orient Bio Inc. (Sungnam, Gyeonggi, South Korea). The mock, *MIR133A* mimic, and *siSOX9* oligonucleotides were prepared and mixed with HCT116 (1×10^7) cells and the cells were injected subcutaneously in nude mice as described previously [11, 12]. Two independent experiments were performed using five mice per each group. The animal studies were approved (WKU17-53) by the Animal Care Committee of the Wonkwang University.

Immunohistochemical analysis

Human colon segments were formalin fixed and paraffin embedded and 5 μm sections were cut for immunohistochemical analysis. The expression of SOX9 was evaluated according to our previously described methods [11, 33].

Western blot analysis

CRC tissues and cells were harvested and lysed in RIPA buffer with protease and phosphatase inhibitor, and protein concentration was measured by BCA protein assay kit (Thermo Scientific). About 30 to 50 μg of protein was loaded and separated through 10-12% Bis-Tris Polyacrylamide gel electrophoresis (PAGE) electrophoretic gel and blotted onto PVDF membranes (Millipore, Burlington, MA, USA). Blots were incubated with primary antibody overnight at 4°C with shaking, then washed with 0.1% T-PBS and incubated with secondary antibody at room temperature for 1 hour. Protein was detected using enhanced chemiluminescence (Millipore). The primary antibodies used were SOX9 (#82630), PIK3CA (#4292), BAX (#2772), Caspase-9 (#9502), pAKT1 (#9271), MAPK1/3 (#4696), CDH1 (#3195) cell signaling. Next, MAP2K1 (sc-219), CDH2 (sc-8424), BCL2 (sc-7382), GAPDH (sc-47724) were from Santa Cruz Biotechnology (Dallas, TX, USA), CTNNB1 (610153) was from BD Biosciences (Franklin Lakes, NJ, USA), and GSK3β (NBp1-47470) was from Novus Biologicals (Englewood, CO, USA). The protein was expression was quantified using Image J software (version 1.44; https://imagej.nih.gov/ij/index.html).

Statistical analysis

The experiments were performed three times using an independent data set with identical results. The data are presented as means ±

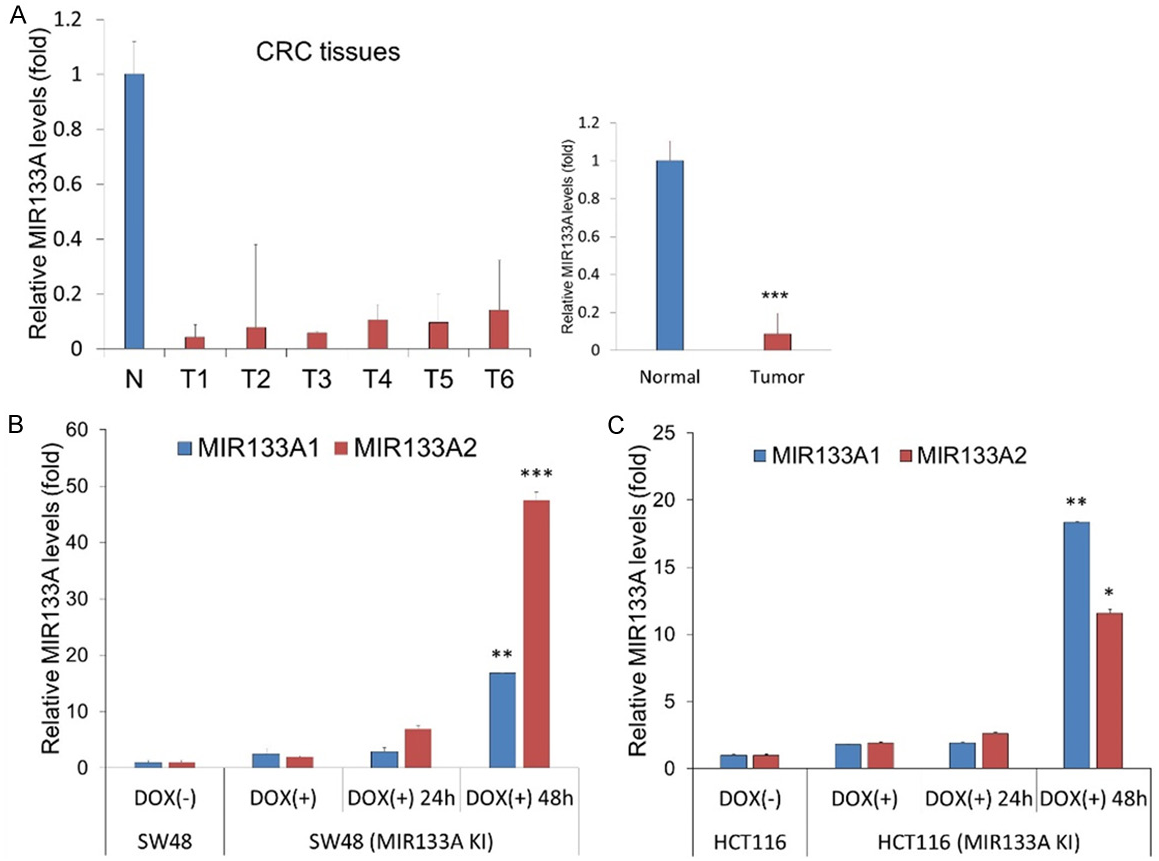

Figure 1. The endogenous *MIR133A* expression in colon cancer tissues and *MIR133A*-overexpressing CRC cells. A. The expression of *MIR133A* was validated using six colon cancer tissue samples and matching adjacent healthy colon tissue samples. The relative expression of *MIR133A* was normalized to colon-specific RNU48. The data are presented as the relative levels (ΔΔCT method) of *MIR133A* in colon cancer tissue. T1, T2, T3, T4, T5, and T6 indicate the tumor sites of patients with colon cancer. B, C. The relative endogenous *MIR133A* expression level in *MIR133A1* and *A2* overexpressed SW48 and HCT116 cell lines. Data are presented as mean ± SD. (**P<0.01, ***P<0.001).

standard deviations (S.D.). All statistical analyses were performed with Excel (Microsoft, Redmond, WA, USA) and GraphPad Prism 8 (one-way analysis of variance [ANOVA]). Two-tailed student t-test or Tukey's test was used to compare multiple data sets. *P*-values <0.05 were considered statistically significant.

Results

MIR133A expression level in colon cancer tissues

We determined the endogenous *MIR133A* level and total RNA for miRNA analysis from 6 pairs of CRC tissues and matching adjacent healthy tissues using TaqMan qRT-PCR. The level of *MIR133A* expression was significantly decreased in CRC tissues (**Figure 1A**).

MIR133A expression level in MIR133A1 and A2 knock-in (KI) cells

We next established the stable *MIR133A1* and *A2* knock-in SW48 and HCT116 cell lines. Knock-in cells were harvested and the total RNA was extracted and analyzed using TaqMan qRT-PCR. As expected, the level of *MIR133A* was significantly increased after 48 hours of doxycycline treatment in *MIR133A1* and *A2* KI SW48 and HCT116 cells (**Figure 1B**, **1C**). Thus, the miRNA expression results show that stable *MIR133A* knock-in CRC cell lines were successfully created.

Identification of MIR133A target genes

Next, to identify the target genes of *MIR133A*, transcriptome analysis was performed using

Table 1. The putative target genes of MIR133A1 identified by the transcriptome analysis from the MIR133A1 Knock-in cells and predicted by the bioinformatics tools

	Gene Symbol	transcript	Description	Fold change*	*P*-value
1	ABHD16A	NM_001177515	abhydrolase domain containing 16A	0.69	0.0322
2	ACAT2	NM_005891	acetyl-CoA acetyltransferase 2	0.59	0.008
3	CALM1	NM_006888	calmodulin 1 (phosphorylase kinase, delta)	0.79	0.0344
4	CDH3	NM_001793	cadherin 3	0.77	0.0449
5	EFNA3	NM_004952	ephrin A3	0.33	0.0007
6	EIF4A1	NM_001416	eukaryotic translation initiation factor 4A1	0.79	0.0289
7	EMP2	NM_001424	epithelial membrane protein 2	0.72	0.0457
8	ENDOD1	NM_015036	endonuclease domain containing 1	0.73	0.0054
9	FOXQ1	NM_033260	forkhead box Q1	0.09	0.001
10	GID8	NM_017896	GID complex subunit 8 homolog	0.74	0.0194
11	GLS2	NM_001280798	glutaminase 2	0.66	0.0202
12	HPGD	NM_000860	hydroxyprostaglandin dehydrogenase 15-(NAD)	0.8	0.0334
13	ISOC2	NM_024710	isochorismatase domain containing 2	0.79	0.0391
14	LY6E	NM_002346	lymphocyte antigen 6 complex, locus E	0.69	0.0149
15	MRPL35	NM_145644	mitochondrial ribosomal protein L35	0.72	0.0109
16	PFDN2	NM_012394	prefoldin subunit 2	0.72	0.0155
17	POLR2J	NM_006234	polymerase (RNA) II subunit J	0.67	0.0361
18	PRPS2	NM_002765	phosphoribosyl pyrophosphate synthetase 2	0.75	0.0001
19	PTPRO	NM_030667	protein tyrosine phosphatase, receptor type O	0.42	0.0051
20	REEP6	NM_138393	receptor accessory protein 6	0.74	0.0263
21	SDC1	NM_001006946	syndecan 1	0.7	0.0438
22	SEC61B	NM_006808	Sec61 translocon beta subunit	0.79	0.0327
23	SNRPE	NM_003094	small nuclear ribonucleoprotein polypeptide E	0.72	0.0302
24	SOX9	NM_000346	SRY-box 9	0.46	0.0035
25	SQLE	NM_003129	squalene epoxidase	0.79	0.0094
26	TAGLN2	NM_003564	transgelin 2	0.7	0.0132
27	TCF7	NM_003202	transcription factor 7	0.58	0.0127
28	TIMM17A	NM_006335	translocase of inner mitochondrial membrane 17 homolog A (yeast)	0.79	0.0242
29	ZDHHC18	NM_032283	zinc finger DHHC-type containing 18	0.77	0.0215

*1.25 fold down, P<0.05 & bioinformatics algorithms.

the independent eight samples (wild SW48 cells, *MIR133A*1 KI SW48 cells, and *MIR133A*2 KI SW48 cells with duplicate). We identified 713 genes whose levels were 1.25-fold down-regulated with P<0.05 levels in *MIR133A*1 KI and *MIR133A*2 KI cells (Table S2). These genes were compared with the candidate *MIR-133A* target genes predicted by the bioinformatics tools (TargetScan, miRanda, and miRWalk algorithms). Of the 713 genes, 29 and 33 putative target genes of *MIR133A1* and *A2*, respectively, were finally identified (**Tables 1**, **2**). Of these, we focused on the master transcription regulator gene *SOX9*.

SOX9 is a direct target of MIR133A

To confirm a direct interaction between the *SOX9* 3'-UTR and *MIR133A*, we cloned wild type (WT) *SOX9* 3'-UTR (predicted to interact with *MIR133A*) into luciferase reporter vector (**Figure 2A**). The luciferase activity of *MIR133A* mimic-transfected cells was significantly decreased compared to wild type in both CRC cell lines (SW48 and Caco2) (**Figure 2B**, **2C**). A *MIR1* mimic (instead of *MIR133A*) was co-transfected with the WT *SOX9* 3'-UTR construct as a negative control. *MIR1* mimic did not affect the luciferase activity of either construct (data not shown). As an additional negative control, we cloned a mutated (MT) version of *SOX9* 3'-UTR whose seven bases complementary to *MIR133A* were deleted (**Figure 2A**). However, the *MIR133A*-mediated inhibition of luciferase activity was abolished by the mutant putative binding site (**Figure 2B**, **2C**). Furthermore, we performed qRT-PCR to measure the expression level of *SOX9* mRNA in *MIR-*

Table 2. The putative target genes of *MIR133A2* identified by the transcriptome analysis from the *MIR133A2* Knock-in cells and predicted by the bioinformatics tools

	Gene Symbol	transcript_id	Description	Fold change*	*P*-value
1	ABHD16A	NM_001177515	abhydrolase domain containing 16A	0.639	0.023
2	ACAT2	NM_005891	acetyl-CoA acetyltransferase 2	0.625	0.008
3	ATOX1	NM_004045	antioxidant 1 copper chaperone	0.711	0.009
4	CALM1	NM_006888	calmodulin 1 (phosphorylase kinase, delta)	0.729	0.011
5	CEBPA	NM_001287435	CCAAT/enhancer binding protein alpha	0.714	0.021
6	CMTM6	NM_017801	CKLF like MARVEL transmembrane domain containing 6	0.782	0.046
7	DOLPP1	NM_001135917	dolichyldiphosphatase 1	0.760	0.039
8	DPM2	NM_003863	dolichyl-phosphate mannosyltransferase polypeptide 2	0.776	0.018
9	EFNA3	NM_004952	ephrin A3	0.310	0.001
10	EIF4A1	NM_001416	eukaryotic translation initiation factor 4A1	0.750	0.004
11	EMP2	NM_001424	epithelial membrane protein 2	0.760	0.014
12	ENDOD1	NM_015036	endonuclease domain containing 1	0.665	0.002
13	FAIM	NM_001033030	Fas apoptotic inhibitory molecule	0.763	0.020
14	FOXQ1	NM_033260	forkhead box Q1	0.090	0.001
15	FTL	NM_000146	ferritin, light polypeptide	0.774	0.024
16	GLS2	NM_001280798	glutaminase 2	0.698	0.016
17	HPGD	NM_000860	hydroxyprostaglandin dehydrogenase 15-(NAD)	0.692	0.044
18	ISOC2	NM_024710	isochorismatase domain containing 2	0.650	0.004
19	LY6E	NM_002346	lymphocyte antigen 6 complex, locus E	0.615	0.014
20	MRPL35	NM_145644	mitochondrial ribosomal protein L35	0.774	0.013
21	NCEH1	NM_020792	neutral cholesterol ester hydrolase 1	0.711	0.016
22	NUBP1	NM_002484	nucleotide binding protein 1	0.779	0.014
23	PRPS2	NM_002765	phosphoribosyl pyrophosphate synthetase 2	0.741	0.003
24	PTPRO	NM_030667	protein tyrosine phosphatase, receptor type O	0.396	0.009
25	SDC1	NM_001006946	syndecan 1	0.650	0.038
26	SERBP1	NM_015640	SERPINE1 mRNA binding protein 1	0.781	0.009
27	SOX9	NM_000346	SRY-box 9	0.391	0.002
28	TAGLN2	NM_003564	transgelin 2	0.626	0.000
29	TCF7	NM_003202	transcription factor 7	0.621	0.019
30	TIMM17A	NM_006335	translocase of inner mitochondrial membrane 17 homolog A (yeast)	0.721	0.019
31	TPD52L1	NM_001300994	tumor protein D52-like 1	0.709	0.010
32	TPM4	NM_001145160	tropomyosin 4	0.778	0.016
33	ZDHHC18	NM_032283	zinc finger DHHC-type containing 18	0.778	0.007

*1.25 fold down, P<0.05 & bioinformatics algorithms.

133A to mimic various transfected CRC cell lines (SW48, Caco2, and SW480 cells). *SOX9* mRNA level was significantly decreased compared with normal mock cells (**Figure 2D**). Likewise, the cellular SOX9 protein was significantly reduced in *MIR133A* mimic-transfected CRC cell lines (SW48, SW480, and HCT116 cells). However, the expression of SOX9 in *MIR133A*-overexpressed Caco2 cells was unaffected (**Figure 2E**).

We also performed qRT-PCR to measure the expression level of *SOX9* mRNA in *MIR133A*1 and *A2* KI SW48 cells. *SOX9* mRNA level was significantly decreased compared with normal mock cells (Figure S1A). Likewise, the cellular SOX9 protein was significantly reduced in *MIR133A1* and *A2* KI SW48 and HCT116 cells (Figure S1B).

Collectively, these results suggest that *SOX9* is a direct target of *MIR133A*. For further study, we selected only two cell lines (SW48 and HCT116) because we could create two stable *MIR133A1* and *A2* KI CRC cell lines in our laboratory. Also, they exhibited consistent mRNA and protein expression when transfected with *MIR133A*.

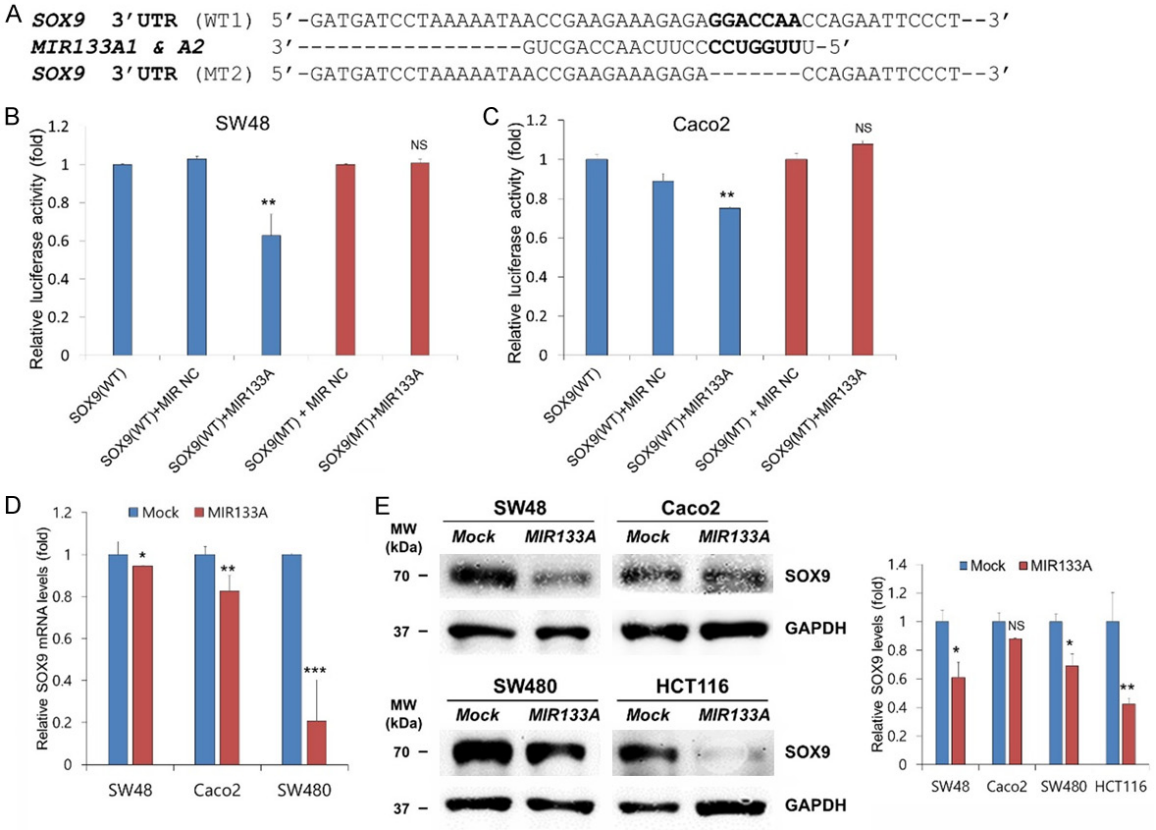

Figure 2. *SOX9* is a direct target of *MIR133A*. A. Sequence alignment of wild-type (WT) and mutant (MT) *MIR133A* target site in the 3'-UTR of *SOX9*. A human *SOX9* 3'-UTR containing the wild-type and mutant *MIR133A* binding sequence was cloned downstream of the luciferase reporter gene. B, C. A luciferase reporter plasmid containing the WT or MT *SOX9* 3'-UTR was co-transfected into SW48 and Caco2 cells with pre-*MIR1* as a negative control or pre-*MIR133A*. Luciferase activity was determined using the dual luciferase assay. Results are shown as relative firefly luciferase activity normalized to Renilla luciferase activity. D. qRT-PCR analysis of *SOX9* expression in SW48, Caco2, and SW480 cells. E. *MIR133A* overexpression decreased SOX9 protein expression in HCT116, SW48, SW480, and Caco2 cell lines. The protein levels of SOX9 were determined by western blotting and densitometry by using Image J, where GAPDH was used as a loading control. Representative data from at least three independent experiments are shown. Each bar represents mean fold alternation above or below control (± SD). Differences were considered as statistically significant $^{*}P<0.05$, $^{**}P<0.01$ compared with control (ns = not significant).

SOX9 expression in human CRC tissues

In line with the above finding, we next evaluated SOX9 expression in six human CRC tissues and the matching healthy colon tissue by western blot and an additional four human CRC tissue pairs by immunohistochemistry. As anticipated, the expression of SOX9 protein was significantly increased in all colon cancer tissues compared to the healthy colon tissues (**Figure 3A**, **3B**).

MIR133A regulates SOX9 and its downstream PIK3CA pathway molecules in CRC cell lines

More recently, it was reported that SOX9 activates the MAPK/ERK pathway (also known as the RAS-RAF-MEK-ERK pathway) via binding to the promoter region of MEK/ERK, while it also activates EMT, apoptosis, and the PIK3CA/AKT pathway and vice versa [18, 34, 35]. Additionally, SOX9 regulates the Wnt/CTNNB1 pathway by increasing GSK-3β phosphorylation or interacting with catenin beta 1 (CTNNB1) [18]. Therefore, we speculated on the molecular and functional cross-talks between *MIR133A*, SOX9, and their downstream molecules in this study. Our western blot results revealed that overexpression of *MIR133A* reduced the direct downstream molecules of SOX9: phosphatidylinositol-4, 5-bisphosphate 3-kinase catalytic subunit alpha (PIK3CA, also known as PI3K), mitogen-activated protein kinase 1 (MAP2K1, also known as MEK1 and MAPKK1), and cad-

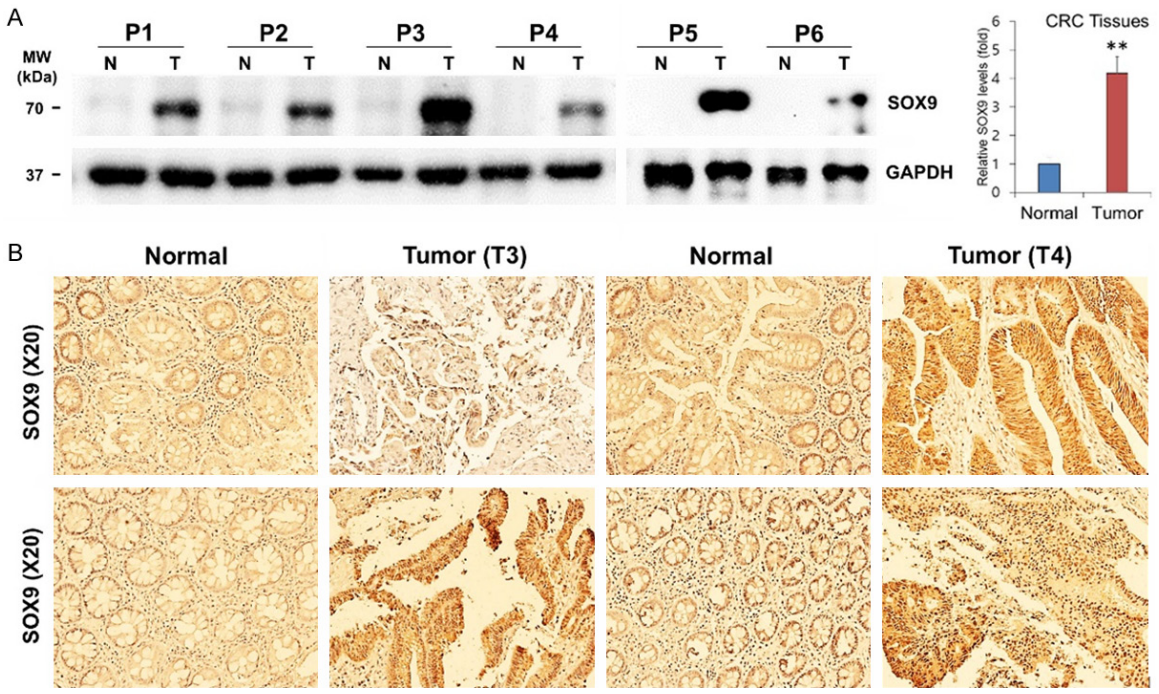

Figure 3. Endogenous SOX9 levels in human CRC tissues. A. The expression levels of SOX9 were validated using 6 pairs of human CRC and adjacent healthy colorectal samples by western blotting and densitometry using Image J, where GAPDH was used as a loading control. Each bar represents mean fold alternation above or below control (± SD). Differences were considered statistically significant $^{**}P<0.01$ compared with control. B. Immunostaining of SOX9 in human CRC tissues and adjacent healthy colorectal samples. Experiments were independently performed three times in duplicate.

herin 2 (CDH2; also known as N-cadherin); however, this change was not statistically significant for PIK3CA in HCT116 cells (**Figure 4A**). On the other hand, the expression level of BCL2 associated X, apoptosis regulator (BAX, also known as BCL2L4) was upregulated by *MIR133A* overexpression (**Figure 4A**).

Since we found that the direct downstream molecules of SOX9 were markedly downregulated in *MIR133A*-overexpressed CRC cell lines, we next investigated their particular downstream pathways. We first examined PIK3CA, AKT serine/threonine kinase 1 (AKT1), glycogen synthase kinase 3 beta (GSK3B, also known as GSK-3β), and CTNNB1. Our western blot results show that *MIR133A* overexpression reduced PIK3CA and pAKT1 protein expression, but this change was not statistically significant in the HCT116 cell line. However, CTNNB1 was statistically reduced (**Figure 4B**). Meanwhile, these proteins were more significantly reduced in the SW48 cell line (**Figure 4B**). Furthermore, in *MIR133A*-overexpressed HCT116 and SW48 cell lines, the expression level of GSK3B was reversed (**Figure 4B**). We then transfected *siSOX9* into HCT116 and SW48 cell lines to see if SOX9 regulates its downstream PIK3CA/AKT1 and GSK3B/CTNNB1 pathways in CRC cells. Western blot results revealed that SOX9 and its downstream components PIK3CA, pAKT1, and CTNNB1 were considerably downregulated by *SOX9* gene silencing, however *siSOX9* had the opposite effect on GSK3B (**Figure 4C**).

MIR133A regulates SOX9 and its downstream MAPK pathways in CRC cell lines

The KRAS (KRAS proto-oncogene, GTPase; also known as K-RAS and RASK2)-BRAF (B-Raf proto-oncogene, serine/threonine kinase, also known as B-RAF and RAFB1)-mitogen-activated protein kinase 1 (MAP2K1; also known as MEK1)-MAPK1 (mitogen-activated protein kinase 1; also known as ERK2, p38, and p40) signaling cascade is a key signaling pathway in cancer development and progression [36, 37]. To explore the expression levels of KRAS downstream molecules by *MIR133A*, we transfected

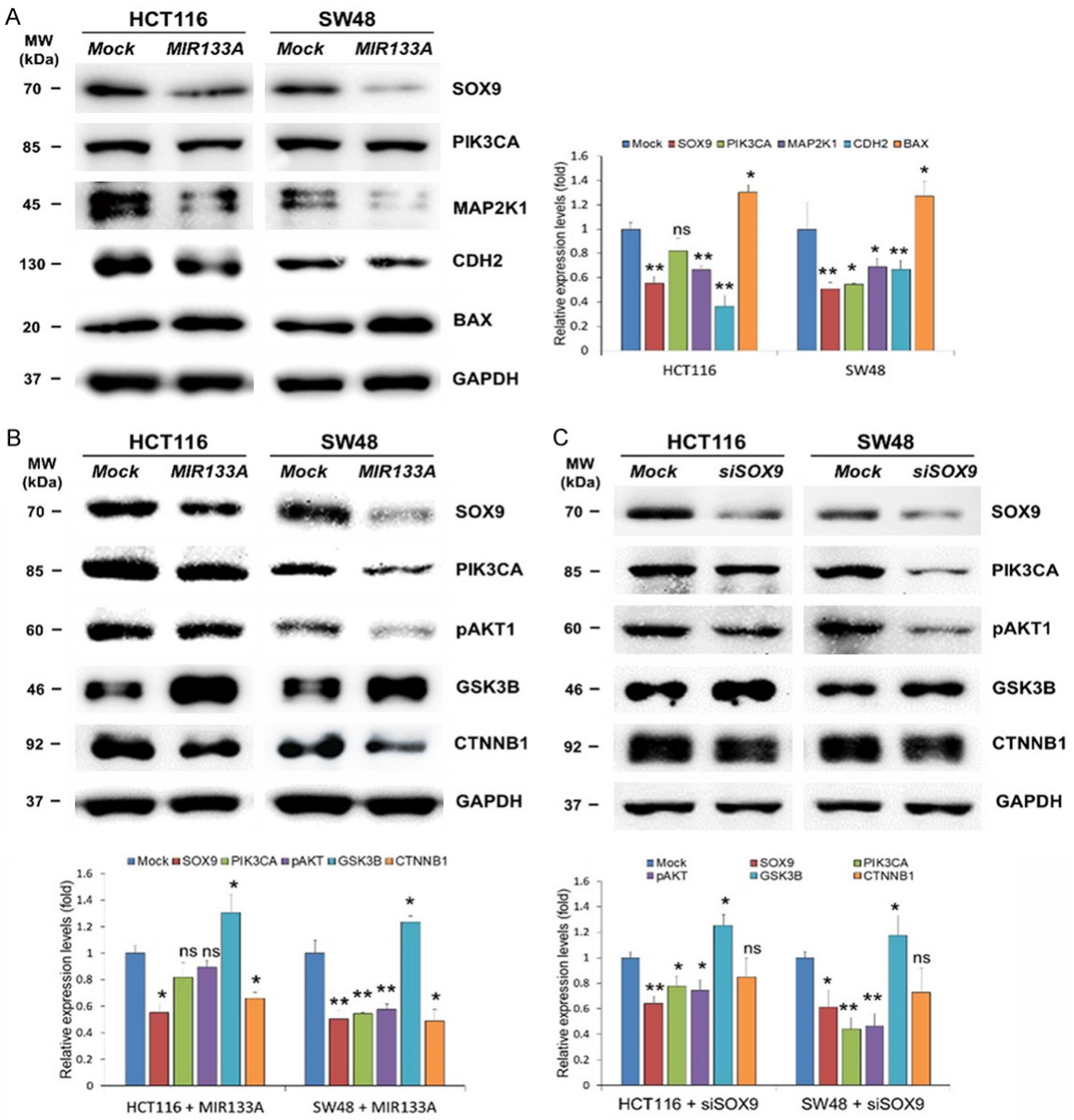

Figure 4. *MIR133A* regulates SOX9 and its downstream PIK3CA pathway molecules in CRC cell lines. A. Western blot analysis of SOX9 and downstream PIK3CA, MAP2K1, CDH2, and BAX in HCT116 and SW48 cells transfected with MIR133A mimic. B. Western blot analysis of SOX9 and its downstream PIK3CA-pAKT1-GSK3B-CTNNB1 in HCT116 and SW48 cells transfected with *MIR133A* mimic. C. SOX-9 and its downstream PIK3CA-pAKT1-GSK3B-CTNNB1 in HCT116 and SW48 cells transfected with *siSOX9*. The protein levels of respective genes were determined by western blotting and densitometry using Image J, where GAPDH was used as a loading control. The representative data from at least three independent experiments are shown. Each bar represents mean fold alternation above or below control (± SD). Differences were considered statistically significant $^{*}P<0.05$, $^{**}P<0.01$ compared with control (ns = not significant).

MIR133A mimic in HCT116 and SW48 cells. Western blot analysis was performed using cells isolated 72 hours after transfection. The expression levels of SOX9 and KRAS downstream molecules were significantly reduced by *MIR133A* overexpression (**Figure 5A**). Additionally, we transfected the *SOX9* siRNA and the negative control into HCT116 and SW48 CRC cell lines, and our western blot results suggest that SOX9 and KRAS downstream proteins were significantly reduced in *siSOX9*-transfected cells (**Figure 5B**).

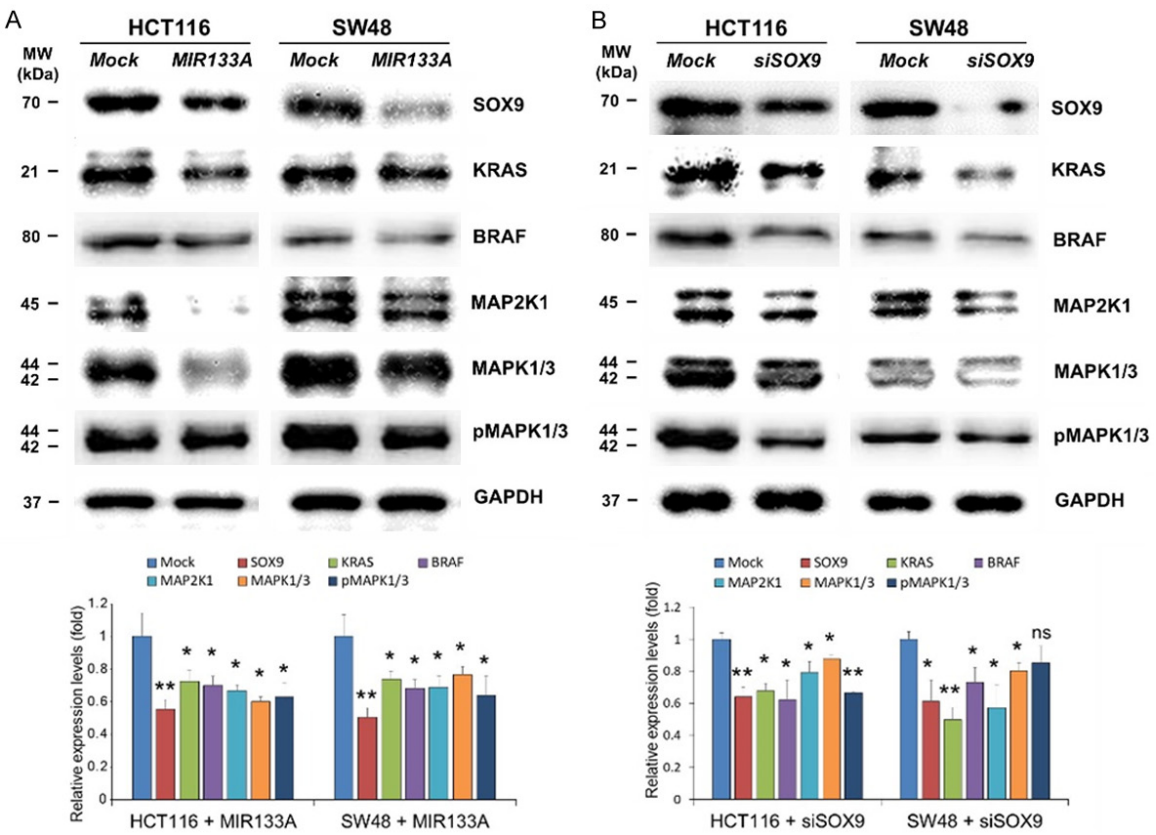

Figure 5. *MIR133A* regulates SOX9-mediated downstream MAPK pathways in CRC cell lines. A. Western blot analysis of SOX9 and its downstream KRAS-BRAF-MAP2K1-MAP2K1/3-pMAP2K1/3 in HCT116 and SW48 cells transfected with MIR133A mimic. B. SOX9 and its downstream KRAS-BRAF-MAP2K1-MAP2K1/3-pMAP2K1/3 in HCT116 and SW48 cells transfected with *siSOX9*. The protein levels of respective genes were determined by western blotting and densitometry using Image J, where GAPDH was used as a loading control. Representative data from at least three independent experiments are shown. Each bar represents mean fold alternation above or below control (± SD). Differences were considered statistically significant $^{*}P<0.05$, $^{**}P<0.01$ compared with control (ns = not significant).

MIR133A regulates SOX9 and its downstream EMT pathways in CRC cell lines

To further rule out the clinical roles of SOX9 in invasion and cancer metastasis, we monitored the expression of EMT markers cadherin 1 (CDH1; also known as E-cadherin) and CDH2. Down-regulation of epithelial marker CDH1 and up-regulation of mesenchymal marker CDH2 is the hallmark of EMT progress [38]. Likewise, our western blot results showed that the expression of CDH1 was not changed in *MIR133A*-overexpressed or *siSOX9*-transfected groups compared to their corresponding control groups (**Figure 6A**, **6B**). In contrast, the expression level of CDH2 was significantly downregulated in CRC cells transfected with *MIR133A* or *siSOX9* (**Figure 6A**, **6B**). Therefore, these findings suggest that ectopic expression of *MIR133A* can suppress EMT via SOX9-mediated pathways and inhibit cellular metastasis.

Effect of MIR133A or SOX9 siRNA transfection on apoptosis in colorectal cancer cells

To elucidate the potential molecular signaling pathway underlying the effect of *MIR133A* on apoptosis of CRC cell lines, we examined the expression of BCL2 apoptosis regulator (BCL2), BAX, and caspase 9 (CASP9) by western blot. As shown in **Figure 7A**, *MIR133A* overexpression in both HCT116 and SW48 cell lines decreased the expression levels of BCL2 but led to a marked increase in the expression level of BAX and the cleaved form of CASP9. To further clarify the *MIR133A*- or SOX9-mediated apoptosis pathway in CRC cell lines, we conduct *SOX9* gene silencing in HCT116 and SW48 cell lines. Immunoblotting results indi-

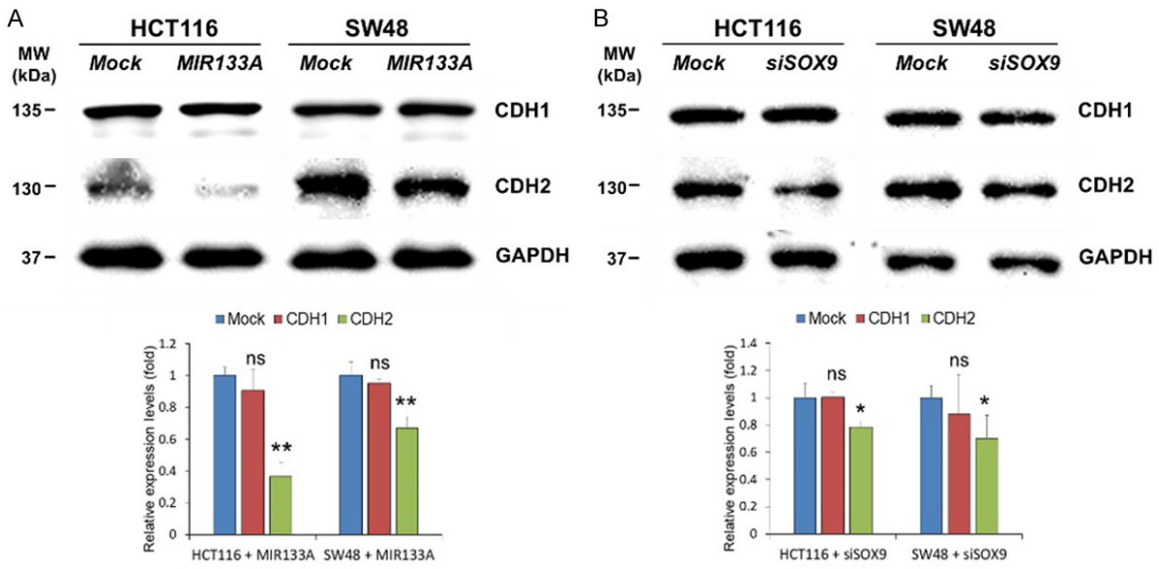

Figure 6. *MIR133A* regulates SOX9 and CDH1-CDH2 expression in CRC cell lines. A. Western blot analysis of SOX9 and CDH1-CDH2 in HCT116 and SW48 cells transfected with *MIR133A* mimic. B. SOX9 and its downstream CDH1-CDH2 in HCT116 and SW48 cells transfected with siSOX9. The protein levels of respective genes were determined by western blotting and densitometry using Image J, where GAPDH was used as a loading control. Representative data from at least three independent experiments are shown. Each bar represents mean fold alternation above or below control (± SD). Differences were considered statistically significant $^{*}P<0.05$, $^{**}P<0.01$ compared with control (ns = not significant).

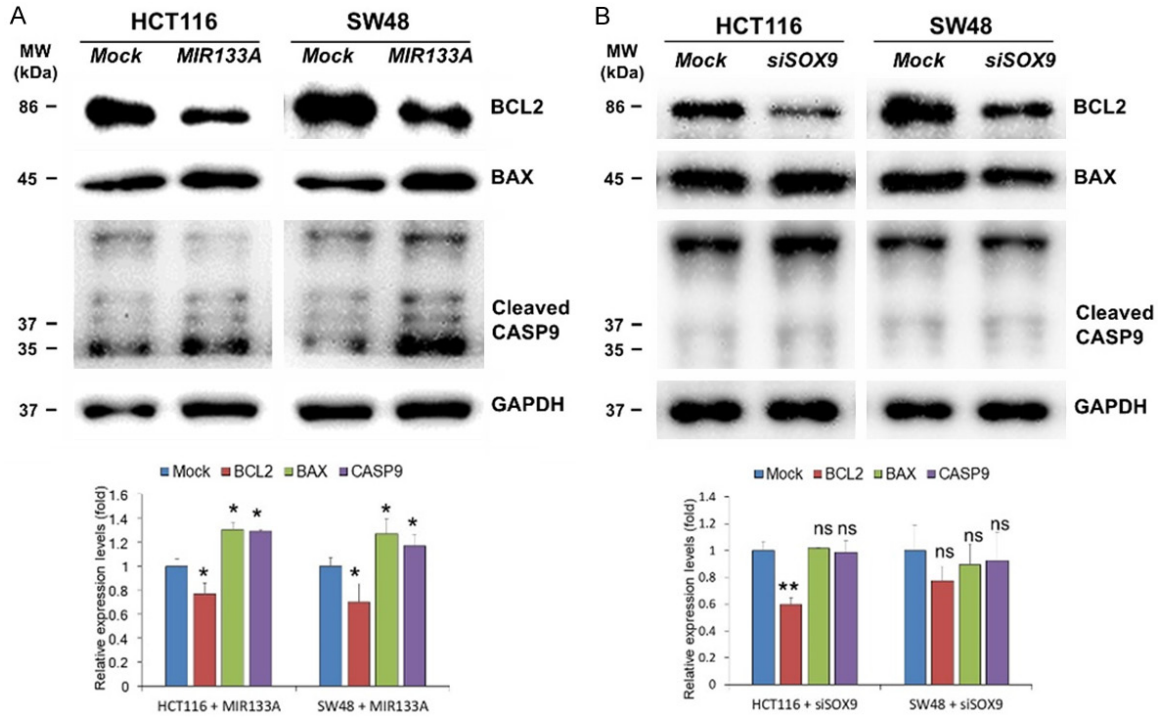

Figure 7. *MIR133A* regulates SOX9 and apoptosis pathways in CRC cell lines. A. Western blot analysis of BCL2, BAX, and cleaved CASP9 in HCT116 and SW48 cells transfected with *MIR133A* mimic. B. BCL2, BAX, and cleaved CASP9 in HCT116 and SW48 cells transfected with *siSOX9*. The protein levels of respective genes were determined by western blotting and densitometry using Image J, where GAPDH was used as a loading control. Representative data from at least three independent experiments are shown. Each bar represents mean fold alternation above or below control (± SD). Differences were considered statistically significant $^{*}P<0.05$, $^{**}P<0.01$ compared with control (ns = not significant).

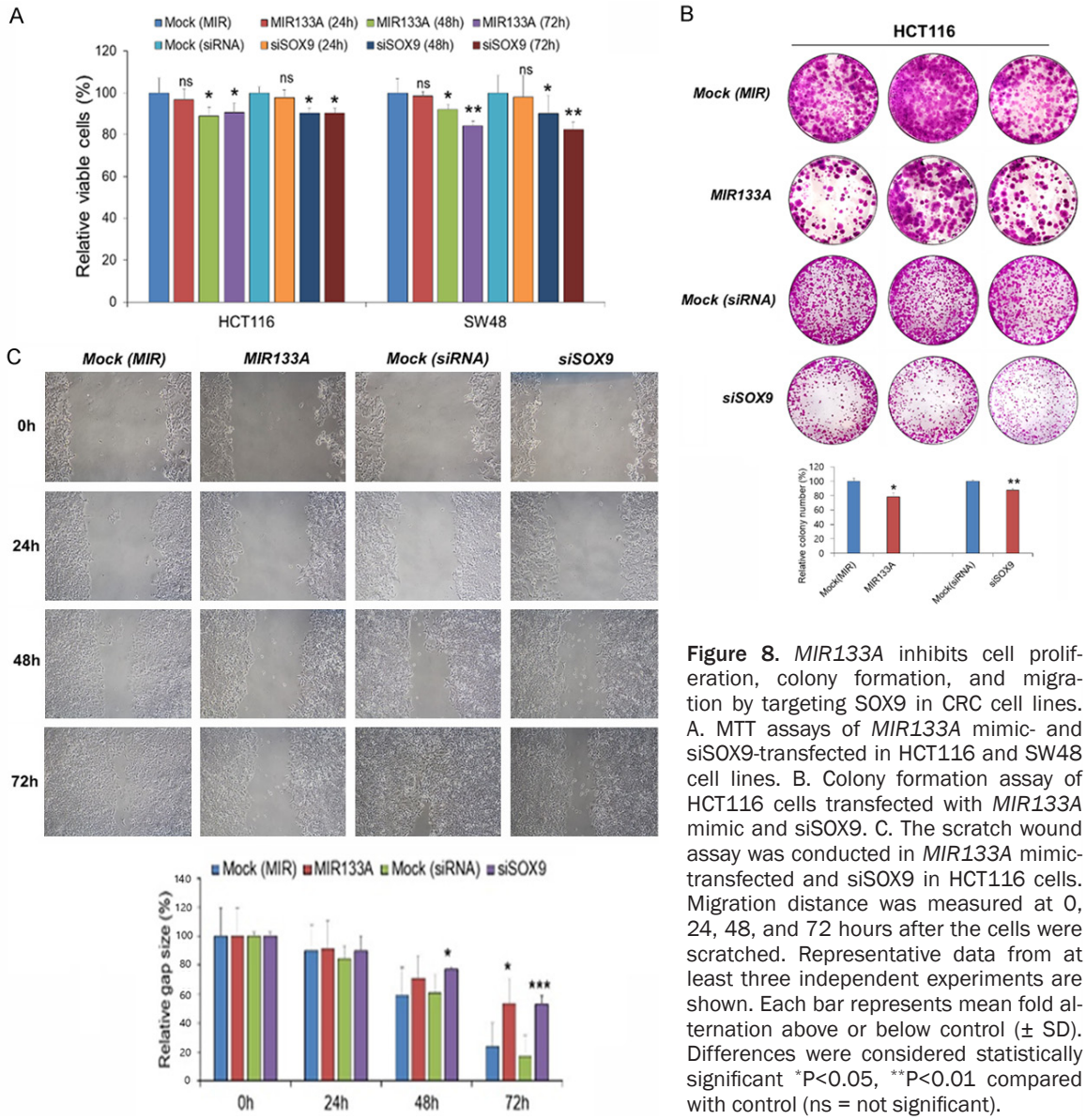

Figure 8. *MIR133A* inhibits cell proliferation, colony formation, and migration by targeting SOX9 in CRC cell lines. A. MTT assays of *MIR133A* mimic- and siSOX9-transfected in HCT116 and SW48 cell lines. B. Colony formation assay of HCT116 cells transfected with *MIR133A* mimic and siSOX9. C. The scratch wound assay was conducted in *MIR133A* mimic-transfected and siSOX9 in HCT116 cells. Migration distance was measured at 0, 24, 48, and 72 hours after the cells were scratched. Representative data from at least three independent experiments are shown. Each bar represents mean fold alternation above or below control (± SD). Differences were considered statistically significant $^{*}P<0.05$, $^{**}P<0.01$ compared with control (ns = not significant).

cated that the SOX9 pathway regulates only BCL2 while the expression of BAX and cleaved CASP9 was not affected by *siSOX9* transfection (**Figure 7B**).

MIR133A inhibits cell proliferation and colony formation in CRC cell lines

To investigate the effect of *MIR133A* on cell proliferation, an MTT assay was performed. Our results demonstrated that transfection of *MIR133A* mimic or *SOX9* siRNA in HCT116 and SW48 cell lines significantly inhibits cell proliferation compared to the control group. Cell viability was not changed in 24 hours, but there was significant inhibition of cell viability after 48 hours and 72 hours in both *MIR133A*- and *siSOX9*-transfected CRC cell lines (**Figure 8A**). Also, there was significant inhibition (48 hours) of cell proliferation in *MIR133A1* and *A2* KI stable HCT116 and SW48 cells compared to the control group (Figure S2). Furthermore, the colony formation assay demonstrated that the colony number of CRC cell lines transfected with *MIR133A* and *siSOX9* was significantly reduced compared with negatively controlled transfected groups (**Figure 8B**). These results suggest that *MIR133A* inhibits cell proliferation and colony formation ability in CRC cell lines by targeting SOX9.

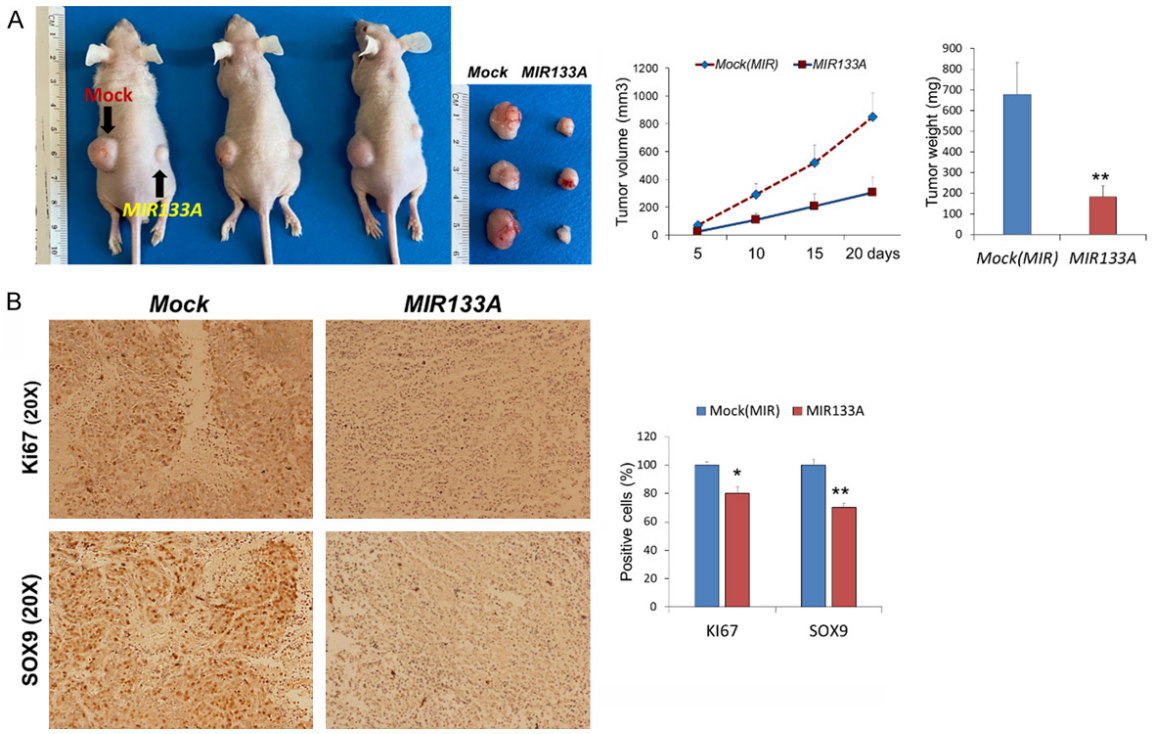

Figure 9. *MIR133A* inhibits xenograft tumor formation of colon cancer cells in mice. *MIR133A* inhibits colon cancer cell growth in vivo. A. Tumor volume, tumor weight and xenograft image of mock or *MIR133A*-transfected HCT116 cells in nude mice. B. Expression of SOX9 and proliferation marker Ki-67 in tumors after subcutaneous transplantation of mock or *MIR133A* in HCT116 cell lines. (n=10, Mean ± SD). Differences were considered statistically significant $^{*}P<0.05$, $^{**}P<0.01$ compared with control.

MIR133A inhibits migration ability of HCT116 by regulating SOX9

Next, to study the potential anti-tumor activity of *MIR133A*, HCT116 cells were transfected with *MIR133A* mimic and *siSOX9*. As shown in the scratch wound assay, the migratory cell ability was significantly inhibited in *MIR133A*-transfected groups compared to the control group. The migratory ability of *MIR133A*-transfected HCT116 cells was significantly inhibited 72 hours after the transfection (**Figure 8C**). Likewise, the cells transfected with *SOX9* siRNA also showed similar results as the migration ability was significantly inhibited after 72 hours of *siSOX9* transfection (**Figure 8C**). These data suggested that *MIR133A* inhibits migration by regulating SOX9.

MIR133A inhibits tumor growth in xenografts

As shown above, transfection with *MIR133A* and *siSOX9* decreased cell proliferation, colony formation, and migratory ability in CRC cell lines. We next investigated the role of *MIR133A* in vivo. We subcutaneously implanted HCT-116 (1×10^7) cells with the overexpression of *MIR133A* in nude mice and monitored tumor cell xenograft formation and growth in every 5 days' interval. Mice were sacrificed on day 20 of transfection, and tumors were harvested. Our results showed that overexpression of *MIR133A* significantly suppressed the growth of CRC cancer xenografts and decreased tumor volume and tumor weight in nude mice (**Figure 9A**). The tumors were analyzed histologically using Ki67 antibody for cellular proliferation, and we found that *MIR133A*-transfected tumors contained a significantly decreased number of Ki67-positive cells compared with mock control tumors for HCT116 cells (**Figure 9B**). *MIR133A* mimic-transfected tumors contained significantly decreased SOX9 expression than mock control tumors (**Figure 9B**). These results indicate that proliferative ability was reduced by *MIR133A* overexpression.

Discussion

Over the last two decades, several studies on miRNAs have shed light on their potential role

in the development and progression of cancers. It is well accepted that miRNAs participate in various biological functions such as cell cycle, cellular proliferation, migration, invasion, apoptosis, and differentiation, and they are anticipated to be a novel diagnostic tool and stable biomarker for cancer detection [11, 39]. Therefore, in this study, we verified the association between *MIR133A* and *SOX9* in CRC cells and tissues and identified novel molecular networks regulated by *MIR133A*, which could add potential therapeutic avenues.

MIR133A expression has been reported to be downregulated in a variety of cancers, including colon cancer [40]. Our findings are consistent with earlier findings that *MIR133A* expression in human colon cancer tissue is significantly lower than in healthy colon tissue (**Figure 1A**). Furthermore, we established two stable *MIR-133A1* and *A2* KI SW48 and HCT116 cell lines to study gene function and elucidate the molecular mechanism. After 48 hours of doxycycline treatment, endogenous *MIR133A* was significantly increased in *MIR133A1* and *A2* KI SW48 and HCT116 cell lines, proving that stable *MIR133A* KI CRC cell lines were successfully created (**Figure 1B**, **1C**). The downregulated genes found by transcriptome analysis using *MIR133A1* and *A2* KI SW48 cell lines were compared with the candidate *MIR133A* target genes predicted by bioinformatics tools, and we identified 29 and 33 putative *MIR133A* and *A2* direct target genes, respectively (**Tables 1**, **2**). We confirmed that *SOX9* was a direct target of *MIR133A* using a dual-luciferase reporter assay (**Figure 2B**, **2C**) as well as western blot analysis (**Figure 2E**).

SOX9 is a critical transcription factor that regulates the progression of various diseases, including cancers. It has been reported that aberrant expression of SOX9 promotes carcinogenesis after acquiring genetic mutations, and believed that around 10% of CRC cases arise from SOX9 gene mutations [18]. Similarly, SOX9 acts as an oncogene and has been found to be up-regulated in different types of cancers [41, 42]. As expected, our results also showed similar patterns. The expression of SOX9 was markedly increased in all colon cancer tissue compared to healthy matching colon tissue (**Figure 3A**, **3B**). This provides further evidence that SOX9 expression levels are elevated in CRC and exhibit a proto-oncogenic function.

The relationship between *MIR133A* and *SOX9* in CRC has never been explored. Therefore, in this study, we attempted to analyze the association between *MIR133A*, its target gene *SOX9*, and their downstream signaling pathways in human CRC cells and tissues (**Figures 4**-**7**). Analogous studies have reported that SOX9 has a positive role in activating the PIK3CA-AKT signaling pathway and that its inhibition reduces cell proliferation, invasion, and apoptosis [43, 44]. Likewise, our study showed that SOX9 and its downstream PIK3CA-AKT expression levels were downregulated by *MIR133A* overexpression in CRC cells (**Figure 4B**). These results are consistent with *siSOX9* treatment in CRC cells (**Figure 4C**), indicating that SOX9 levels are inversely correlated with *MIR133A* levels in CRC cells and tissues.

GSK3B-CTNNB1 pathways are considered a PIK3CA-AKT pathway component. The upstream protein kinase AKT, known to phosphorylate and inactivate GSK3, is frequently dysregulated in tumors [45]. It has been observed that phosphorylation of a serine (S9) of GSK3β results in GSK3β inactivation, which then phosphorylates the proto-oncogenic molecule CTNNB1, causing it to be targeted for destruction or inactivation. As a result, transcription of these genes involved in cell growth is inhibited [46]. Based on the preceding information, we further wanted to see if *MIR133A* affects the expression of the GSK3B-CTNNB1 pathway. Our results from *MIR133A* overexpression and SOX9 gene silencing revealed that *MIR133A* downregulated CTNNB1 via the SOX9-mediated pathway. On the other hand, the GSK3B level increased in CRC cell lines when *MIR133A* was overexpressed (**Figure 4B**, **4C**). Similar outcomes were seen when miRNA-302a was overexpressed in prostate cancer, notably the downregulation of pAKT and upregulation of GSK3β [47]. In contrast, upregulation of miRNA-29a decreases PIK3CA, p-AKT, and GSK3β in HCT-116 cell lines [48]. Indeed, the molecular interactions between multiple signaling pathways and the varying roles of GSK3B in these pathways make it extremely difficult to elucidate the exact signaling pathway.

Recent works have demonstrated that *MIR-133A* represses cell proliferation, migration, and invasion by targeting the MEK-ERK signaling pathway in bladder and colorectal cancer [49, 50]. In contrast, there are limited studi-

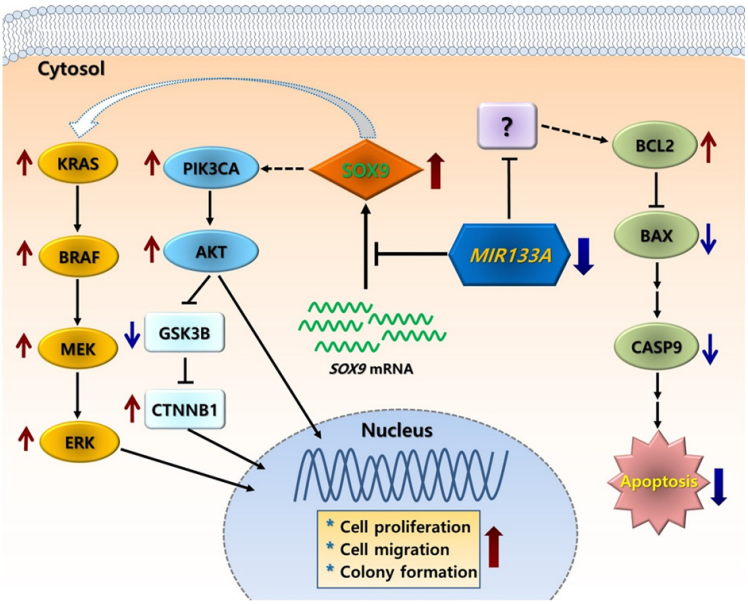

Figure 10. A simple putative mechanism of *MIR133A* regulation of SOX9-mediated cell proliferation, cell migration, and colony formation in human CRC. Decreased *MIR133A* expression in CRC cells or tissues leads to up-regulation of cellular SOX9 levels. The increased SOX9 level causes activation of downstream pathways, such as PIK3CA-pAKT-GSK3B-CTNNB1, KRAS-BRAF-MAP2K1 (MEK)-MAP2K1/3 (ERK), and apoptosis pathways, resulting in increased colony formation, cell proliferation, and cell migration.

es about *MIR133A* and its regulatory effects on KRAS-KRAF upstream of MAP2K1-MAPK1/3 signaling. Hence, we investigated the regulatory relationship between *MIR133A* and the MAP2K1-MAPK1/3 signaling cascade in this study. Our result demonstrated that *MIR133A* overexpression downregulated the MAP2K1-MAPK1/3 signaling cascade in HCT116 and SW48 CRC cell lines (**Figure 5A**). We obtained similar results by silencing the *SOX9* gene in HCT116 and SW48 CRC cell lines (**Figure 5B**). These results suggested that *MIR133A* regulated the *SOX9*-mediated KRAS-BRAF-MAP2K1-MAPK1/3 signaling pathway.

In vivo and *in vitro* data indicates that SOX9 binds to the metastasis-regulator genes or the promoter region of several EMT genes and regulates cancer cell invasion and metastasis [51, 52]. Together with our results, down-regulation of CDH2 was observed by *MIR133A* overexpression or *SOX9* gene silencing in HCT116 and SW48 cell lines (**Figure 6A**, **6B**). It was reported that CASP3 activity, BAX, and cleaved CASP9 expression levels were significantly higher in miR-133a mimic-overexpressed breast cancer cells, although BCL2 expression was reversed [53]. In *MIR133A*-overexpressed CRC cell lines, we found that BAX and cleaved CASP9 expression were significantly increased, while BCL2 expression was decreased (**Figure 7A**). However, *siSOX9* had no effect on BAX or CASP9 (**Figure 7B**). These results indicate that SOX9 may not regulate BAX and CASP9, and there might be other molecules regulated by *MIR133A*. As a result, more research is needed to fully understand the relationship between SOX9, BAX, and CASP9 in colorectal cancer.

After identifying *SOX9* as a direct target of *MIR133A* and demonstrating its underlying molecular mechanism, we performed *in vitro* and *in vivo* functional studies. As anticipated, overexpression of *MIR133A* and *SOX9* gene silencing in CRC cell lines inhibited cell proliferation, as revealed by MTT cell viability (**Figure 8A**), colony formation (**Figure 8B**), and Ki67 immunohistochemistry assay (**Figure 9B**). Next, *in vitro* evidence suggested that *MIR133A* may inhibit CRC cell motility and migration by targeting SOX9 (**Figure 8C**). To confirm the above finding, we carry out an *in vivo* xenograft experiment in nude mice. We found that colon cancer cells overexpressing *MIR133A* suppress tumor growth compared to control cells (**Figure 9A**). The tumor volume and weight were significantly decreased by *MIR133A* overexpression (**Figure 9A**). It is worthy to point out that *MIR133A* is a direct target of *SOX9* and functions as a tumor repressor in colorectal cancer.

Conclusions

Conclusively, we demonstrated that *MIR133A* is downregulated in human CRC tissue. We identified *SOX9* as a putative target gene of *MIR133A* and showed that *SOX9* is a direct target of *MIR133A* in human CRC cells. Our results indicate that *MIR133A* regulates two SOX9-mediated signaling pathways (PIK3CA-AKT1-

GSK3B-CTNNB1 and KRAS-BRAF-MAP2K1-MAPK1/3) and SOX9-mediated BCL2 and CDH2 expression, and as a result, *MIR133A* regulates cell proliferation, cell migration, and colony formation via targeting SOX9 in CRC cells. Although we did not investigate the mechanism of *MIR133A* downregulation in CRC cells, our results overall suggest that the diminished *MIR133A* levels during CRC progression upregulate SOX9 expression. The upregulated intracellular SOX9 levels might, in turn, affect downstream signal pathways. Consequently, they might upregulate cell proliferation, cell migration, and colony formation in CRC (**Figure 10**). Therefore, *MIR133A* might be a promising therapeutic target for cancer diagnosis, prognosis, and treatment.

Acknowledgements

The biospecimens for this study were provided by the Biobank of Wonkwang University Hospital, a member of the National Biobank of Korea, which is supported by the Ministry of Health and Welfare. This work was supported by the National Research Foundation of Korea (NRF) grant funded by the Korea government (MSIT); 2017R1A2B4004801 and 2020R1A2C2003882.

Disclosure of conflict of interest

None.

Address correspondence to: Soo-Cheon Chae, Department of Pathology, School of Medicine, Wonkwang University, Iksan, Chonbuk 54538, Korea. Tel: +82-63-8506793; E-mail: chaesc@wku.ac.kr

References

[1] Hofseth LJ, Hebert JR, Chanda A, Chen H, Love BL, Pena MM, Murphy EA, Sajish M, Sheth A, Buckhaults PJ and Berger FG. Early-onset colorectal cancer: initial clues and current views. Nat Rev Gastroenterol Hepatol 2020; 17: 352-364.

[2] Bray F, Ferlay J, Soerjomataram I, Siegel RL, Torre LA and Jemal A. Global cancer statistics 2018: GLOBOCAN estimates of incidence and mortality worldwide for 36 cancers in 185 countries. CA Cancer J Clin 2018; 68: 394-424.

[3] Xi Y and Xu PF. Global colorectal cancer burden in 2020 and projections to 2040. Transl Oncol 2021; 14: 101174.

[4] Jung G, Hernandez-illan E, Moreire L, Balaguer F and Goel A. Epigenetics of colorectal cancer: biomarker and therapeutic potential. Nat Rev Gastroenterol Hepatol 2020; 17: 111-130.

[5] Sandler RS. Epidemiology and risk factors for colorectal cancer. Gastroenterol Clin North Am 1996; 25: 717-735.

[6] Skarkova V, Kralova V, Vitovcova B and Rudolf E. Selected aspects of chemoresistance mechanisms in colorectal carcinoma-a focus on epithelial-to-mesenchymal transition, autophagy, and apoptosis. Cells 2019; 8: 234.

[7] Ji WD, Sun B and Su CQ. Targeting microRNAs in cancer gene therapy. Genes (Basel) 2017; 8: 21.

[8] Abd-Aziz N, Kamaruzman NI and Poh CL. Development of microRNAs as potential therapeutics against cancer. J Oncol 2020; 2020: 8029721.

[9] Burt R. Inheritance of colorectal cancer. Drug Discov Today Dis Mech 2007; 4: 293-300.

[10] Lu J, Getz G, Miska EA, Alvarez-Saavedra E, Lamb J, Peck D, Sweet-Cordero A, Ebert BL, Mak RH, Ferrando AA, Downing JR, Jacks T, Horvitz HR and Golub TR. MicroRNA expression profiles classify human cancers. Nature 2005; 435: 834-838.

[11] Alam KJ, Mo JS, Han SH, Park WC, Kim HS, Yun KJ and Chae SC. MicroRNA 375 regulates proliferation and migration of colon cancer cells by suppressing the CTGF-EGFR signaling pathway. Int J Cancer 2017; 141: 1614-1629.

[12] Mo JS, Park WC, Choi SC, Yun KJ and Chae SC. MicroRNA 452 regulates cell proliferation, cell migration, and angiogenesis in colorectal cancer by suppressing VEGFA expression. Cancers 2019; 11: 1613.

[13] Dong YJ, Zhao JH, Wu CW, Zhang LJ, Liu XD, Kang W, Leung WW, Zhang N, Chan FK, Sung JJ, Ng SS and YU J. Tumor suppressor functions of miR-133a in colorectal cancer. Mol Cancer Res 2013; 11: 1051-1060.

[14] Gong Y, Ren J, Liu K and Tang LM. Tumor suppressor role of miR-133a in gastric cancer by repressing IGF1R. World J Gastroenterol 2015; 21: 2949-2958.

[15] Chen LJ, He XB, Xie YP, Huang Y, Wolff DW, Abel PW and Tu YP. Up-regulated miR-133a orchestrates epithelial-mesenchymal transition of airway epithelial cells. Sci Rep 2018; 8: 15543.

[16] Gutiérrez NC, Sarasquete ME, Misiewicz-Krzeminska I, Delgado M, De Las Rivas J, Ticona FV, Ferminan E, Martin-Jimenez P, Chillon C, Risueno A, Hernandez JM, Garcia-Sanz R, Gonzalez M and San Miguel JF. Deregulation of microRNA expression in the different genetic subtypes of multiple myeloma and correlation with gene expression profiling. Leukemia 2010; 24: 629-637.

[17] Jana S, Madhu Krishna B, Singhal J, Horne D, Awasthi S, Salgia R and Singhal SS. SOX9: the master regulator of cell fate in breast cancer. Biochem Pharmacol 2020; 174: 113789.
[18] Panda M, Tripathi SK and Biswal BK. SOX9: an emerging driving factor from cancer progression to drug resistance. Biochim Biophys Acta Rev Cancer 2021; 1875: 188517.
[19] Jo A, Denduluri S, Zhang BS, Wang ZL, Yin LJ, Yan ZJ, Kang R, Shi LL, Mok J, Lee MJ and Haydon RC. The versatile functions of Sox9 in development, stem cells, and human diseases. Genes Dis 2014; 1: 149-161.
[20] Wang HY, Leav I, Ibaragi S, Wegner M, Hu GF, Lu ML, Balk SP and Yuan X. SOX9 is expressed in human fetal prostate epithelium and enhances prostate cancer invasion. Cancer Res 2008; 68: 1625-1630.
[21] Lin RX, Zhan GF, Wu JC, Fang H and Yang SL. LncRNA snhg14 sponges mir-206 to affect proliferation, apoptosis, and metastasis of hepatocellular carcinoma cells by regulating sox9. Dig Dis Sci 2022; 67: 936-946.
[22] Huang J and Guo L. Knockdown of SOX9 inhibits the proliferation, invasion, and EMT in thyroid cancer cells. Oncol Res 2017; 25: 167-176.
[23] Santos JC, Carrasco-Garcia E, Garcia-Pug M, Aldaz P, Monte M, Fernandez-Reyes M, de Oliveira CC, Lawrie CH, Araúzo-Bravo MJ, Ribeiro ML and Matheu A. SOX9 elevation acts with canonical WNT signaling to drive gastric cancer progression. Cancer Res 2016; 76: 6735-6746.
[24] Wang HY, Lian P and Zheng PS. SOX9, a potential tumor suppressor in cervical cancer, transactivates p21WAF1/CIP1 and suppresses cervical tumor growth. Oncotarget 2015; 6: 20711-20722.
[25] Mo JS, Alam KJ, Kim HS, Lee YM, Yun KJ and Chae SC. MicroRNA 429 regulates mucin gene expression and secretion in murine model of colitis. J Crohns Colitis 2016; 10: 837-849.
[26] De Sena Brandine G and Smith AD. Falco: high-speed FastQC emulation for quality control of sequencing data. F1000Res 2019; 8: 1874.
[27] Trapnell C, Pachter L and Salzberg SL. TopHat: discovering splice junctions with RNA-Seq. Bioinformatics 2009; 25: 1105-1111.
[28] Roberts A, Trapnell C, Donaghey J, Rinn JL and Pachter L. Improving RNA-Seq expression estimates by correcting for fragment bias. Genome Biol 2011; 12: R22.
[29] R Development Core Team. R: A Language and Environment for Statistical Computing. R Foundation for Statistical Computing, Vienna, 2016.
[30] Han SH, Mo JS, Park WC and Chae SC. Reduced microRNA 375 in colorectal cancer upregulates metadherin-mediated signaling. World J Gastroenterol 2019; 25: 6495-6507.
[31] Lamichhane S, Bastola T, Pariyar R, Lee ES, Lee HS, Lee DH and Seo J. ROS production and ERK activity are involved in the effects of d-β-hydroxybutyrate and metformin in a glucose deficient condition. Int J Mol Sci 2017; 18: 674.
[32] Mo JS, Alam KJ, Kang IH, Park WC, Seo GS, Choi SC, Kim HS, Moon HB, Yun KJ and Chae SC. MicroRNA 196B regulates FAS-mediated apoptosis in colorectal cancer cells. Oncotarget 2015; 6: 2843-2855.
[33] Mo JS, Han SH, Yun KJ and Chae SC. MicroRNA 429 regulates the expression of CHMP5 in the inflammatory colitis and colorectal cancer cells. Inflamm Res 2018; 67: 985-996.
[34] Huang JQ, Wei FK, Xu XL, Ye SX, Song JW, Ding PK, Zhu J, Li HF, Luo XP, Gong H, Su L, Yang L and Gong LY. SOX9 drives the epithelial-mesenchymal transition in non-small-cell lung cancer through the Wnt/β-catenin pathway. J Transl Med 2019; 17: 143.
[35] Stockl S, Bauer BJ, Bosserhoff AK, Gottl C, Grifka J and Grassel S. Sox9 modulates cell survival and adipogenic differentiation of multipotent adult rat mesenchymal stem cells. J Cell Sci 2013; 126: 2890-2902.
[36] Degirmenci U, Wang M and Hu JC. Targeting aberrant RAS/RAF/MEK/ERK signaling for cancer therapy. Cells 2020; 9: 198.
[37] Guo YJ, Pan WW, Liu SB, Shen ZF, Xu Y and Hu LL. ERK/MAPK signalling pathway and tumorigenesis. Exp Ther Med 2020; 19: 1997-2007.
[38] Huang LX, Hu CY, Jing L, Wang MC, Xu M, Wang J, Wang Y, Nan KJ and Wang SH. Micro RNA-219-5p inhibits epithelial-mesenchymal transition and metastasis of colorectal cancer by targeting lymphoid enhancer-binding factor 1. Cancer Sci 2017; 108: 1985-1995.
[39] Kong B, Zhao SP, Kang XW and Wang B. MicroRNA-133a-3p inhibits cell proliferation, migration and invasion in colorectal cancer by targeting AQP1. Oncol Lett 2021; 22: 649.
[40] Li W, Chen A, Xiong L, Chen T, Tao F, Lu Y, He Q, Zhao L, Ou R and Xu Y. miR-133a acts as a tumor suppressor in colorectal cancer by targeting eIF4A1. Tumour Biol 2017; 39: 1010428317698389.
[41] Zhong WD, Qin GQ, Dai QS, Han ZD, Chen SM, Ling XH, Fu X, Cai C, Chen JH, Chen XB, Lin ZY, Deng YH, Wu SL, He HC and Wu CL. SOXs in human prostate cancer: implication as progression and prognosis factors. BMC Cancer 2012; 12: 248.
[42] Lu BJ, Fang YH, Xu J, Wang LP, Xu FY, Xu EP, Huang Q and Lai MD. Analysis of SOX9 expression in colorectal cancer. Am J Clin Pathol 2008; 130: 897-904.

[43] Swartling FJ, Ferletta M, Kastemar M, Weiss WA and Westermark B. Cyclic GMP-dependent protein kinase II inhibits cell proliferation, Sox9 expression and Akt phosphorylation in human glioma cell lines. Oncogene 2009; 28: 3121-3131.
[44] Liu HW, Liu ZX, Jiang B, Peng RJ, Ma ZM and Lu JC. SOX9 overexpression promotes glioma metastasis via Wnt/β-catenin signaling. Cell Biochem Biophys 2015; 73: 205-212.
[45] Robinson JP, Vanbrocklin MW, McKinney AJ, Gach HM and Holmen SL. Akt signaling is required for glioblastoma maintenance in vivo. Am J Cancer Res 2011; 1: 155-167.
[46] Mills CN, Nowsheen S, Bonner JA and Yang ES. Emerging roles of glycogen synthase kinase 3 in the treatment of brain tumors. Front Mol Neurosci 2011; 4: 47.
[47] Zhang GM, Bao CY, Wan FN, Cao DL, Qin XJ, Zhang HL, Zhu Y, Dai B, Shi GH and Ye DW. MicroRNA-302a suppresses tumor cell proliferation by inhibiting AKT in prostate cancer. PLoS One 2015; 10: e0124410.
[48] Han XF, Zhang JW, Wang YL and Gao ZG. miRNA-29a inhibits colon cancer growth by regulation of the PTEN/Akt/GSK3β and Wnt/β-catenin signaling pathways. Oncol Lett 2018; 16: 2638-2644.
[49] Cui WJ, Zhang S, Shan CL, Zhou L and Zhou ZM. micro RNA-133a regulates the cell cycle and proliferation of breast cancer cells by targeting epidermal growth factor receptor through the EGFR/A kt signaling pathway. FEBS J 2013; 280: 3962-3974.
[50] Wang H, An HY, Wang B, Liao Q, Li WD, Jin XJ, Cui SZ, Zhang YJ, Ding YQ and Zhao L. miR-133a represses tumour growth and metastasis in colorectal cancer by targeting LIM and SH3 protein 1 and inhibiting the MAPK pathway. Eur J Cancer 2013; 49: 3924-3935.
[51] Ma YX, Shepherd J, Zhao DK, Bollu LR, Tahaney WM, Hill J, Zhang Y, Mazumdar A and Brown PH. SOX9 is essential for triple-negative breast cancer cell survival and metastasis. Mol Cancer Res 2020; 18: 1825-1838.
[52] Aguilar-Medina M, Avendaño-Félix M, Lizárraga-Verdugo E, Bermúdez M, Romero-Quintana JG, Ramos-Payan R, Ruíz-García E and López-Camarillo C. SOX9 stem-cell factor: clinical and functional relevance in cancer. J Oncol 2019; 2019: 6754040.
[53] Li ZF, Xu WW, Ren XY, Xu JH and Chen JX. Puerarin promotes DUSP1 expression by regulating miR-133a-3p in breast cancer. Mol Med Rep 2019; 19: 205-212.

Table S1. Primer sequences used for MIR133A knock-in, qRT-PCR, luciferase assay and Taq-Man analysis in this study

Applications	Primers*	Primer sequence (5'→3')
Knock-In	MIR133A1-F	CACGGATCCCTAGCAGCACTACAATGC
	MIR133A1-R	CCGAAGCTTGTCCCGTAGTAATCAATGCATA
	MIR133A2-F	TATGGATCCTCCGACGTCGCTGTTC
	MIR133A2-R	TATAAGCTTCACGGCTGCGGGACCT
qRT-PCR	SOX9-QF1	CGAAGATGGCCGAGATGATCC
	SOX9-QR1	GGATAGGTCATGTTTGTGTCTTGG
	GAPDH-F	CAATGACCCCTTCATTGACC
	GAPDH-R	GACAAAGCTTCCCGTTCTCAG
Luciferase assay	SOX9-WF	CGACGAGCTCCTTCACCTACATGAACC
	SOX9-WR	GCTGCTCGAGGTTGCCTTTAGCTTAAATGTC
	SOX9-MF	CCGAAGAAAGAGACCAGAATTCCCTTTGG
	SOX9-MR	CCAAAGGGAATTCTGGTCTCTTTCTTCGG
Taq-Man analysis	Hsa-mir-133A	ID: PM10413 (Applied Biosystems)
	RNU48	GATGACCCCAGGTAACTCTGAGTGTGTCGC
		TGATGCCATCACCGCAGCGCTCTGACC

*QF: quantitative forward primer; QR: quantitative reverse primer; WF: forward primer for wild-type constructs; WR: reverse primer for wild-type constructs; MF: forward primer for mutate-type constructs; MR: reverse primer for mutate-type constructs.

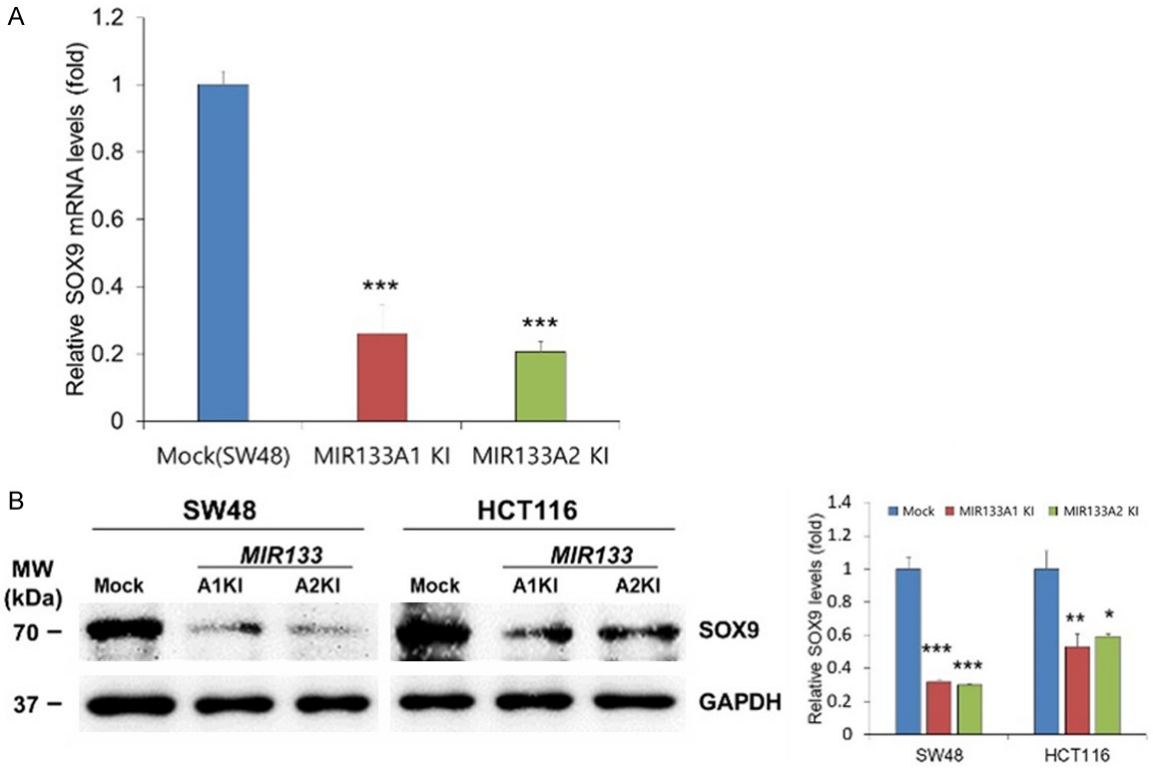

Figure S1. SOX9 mRNA and protein levels and MIR133A1 and A2 KI cell lines. A. qRT-PCR analysis of SOX9 mRNA expression in MIR133A1 and A2 KI SW48 cells relative to mock cells. B. Western blot analysis of SOX9 in MIR133A1 and A2 KI SW48 and HCT116 cells. Differences were considered statistically significant $^{*}P<0.05$, $^{**}P<0.01$, $^{***}P<0.001$ compared with control.

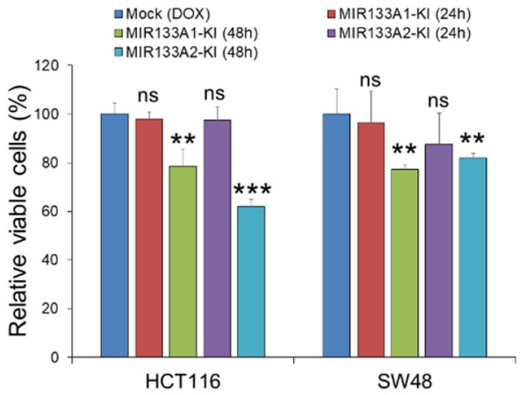

Figure S2. Cell proliferation in MIR133A1 and A2 KI cell lines. MTT assays of mock and MIR133A1 and A2. Representative data from at least three independent experiments are shown. Each bar represents mean fold alternation above or below control (± SD). Differences were considered statistically significant $^{**}P<0.01$, $^{***}P<0.001$ compared with control (ns = not significant).